



Gradient elasticity theories and finite element implementations for static fracture

H. Askes

Department of Civil & Structural Engineering, University of Sheffield (UK)

h.askses@sheffield.ac.uk

ABSTRACT. Gradient elasticity theories are a powerful tool to describe the state of stress and strain around sharp crack tips. With the appropriate format of field equations and boundary conditions, gradient elasticity can be used to predict non-singular stresses and strains, which can aid in simplifying engineering interpretation and the formulation of propagation criteria. The additional terms in the continuum equations are accompanied by internal length scales that represent the microstructure, and these internal length scales may be used to interpret fracture process zones or critical distances in fatigue theory. One of the difficulties of gradient elasticity theories, and the main reason why they have not been disseminated widely in the engineering communities, is that their finite element implementation is not straightforward. However, much progress has been made in recent years, and in this paper a few relatively simple implementations will be shown.

KEYWORDS. Gradient elasticity, generalised continuum, length scale, crack tip singularities, finite elements.

INTRODUCTION

The classical equations of elasticity relate stresses to strains, without including higher-order derivatives of the state variables. Whilst classical elasticity has proven its value in describing phenomena with relatively uniform states of deformation, its use in problems with localised deformations is more problematic. For instance, the stress and strain fields around sharp crack tips or points where concentrated forces are applied are plagued by singularities. The reason for this unphysical feature of classical elasticity is that micro-structural effects are missing in the description. This also implies that classical elasticity is incapable of describing size-dependent response or the dispersion of propagating waves.

As an alternative, one can use *gradient elasticity*. Compared to classical elasticity, the field equations of gradient elasticity are equipped with higher-order spatial derivatives of the relevant variables. The higher-order derivative terms are accompanied by additional constitutive parameters that have the dimension of length, and these parameters represent the underlying micro-structure of the material. There are many different versions of gradient elasticity, the most relevant of which will be discussed below, but with an appropriate format of gradient elasticity it is possible to describe the stresses and strains around sharp cracks without singularities. It is also possible to predict a size-dependent response and to describe dispersive wave propagation, although these two issues are beyond the scope of the present paper.

The earliest systematic attempts at enriching classical elasticity with higher-order micro-structural terms date back to the 19th century, when Cauchy used series expansions to include higher-order derivatives in the equations of elasticity, see for instance [1], and Voigt formulated a continuum theory which included not only displacements but also rotations as independent kinematic variables [2]. In the 1960s, Mindlin developed a complete linear theory of elasticity with micro-structure. Although the full theory is rather complicated and has in its most general format over 900 independent constitutive constants, he also formulated various simplifications based on assumptions of isotropy, symmetry and the coupling of micro-scale and macro-scale kinematic variables [3]. Whereas Mindlin's work was concentrated on introducing



micro-structural influences via additional spatial *gradients*, Eringen focussed on using spatial *integrals* to achieve the same objective. However, in the 1980s Eringen also formulated a differential version of his integral theory [4]. About a decade later, yet another variant of gradient elasticity was suggested by Aifantis [5]. All these theories have in common that they can describe the stresses and strains around sharp crack tips without singularities, which can be of benefit in the interpretation of the crack state and in formulating appropriate propagation criteria.

The gradient theories of Mindlin, Eringen and Aifantis will be reviewed and compared in Section *Overview of pertinent gradient elasticity theories*. A discussion of the internal length scale parameter that accompany the higher-order derivative terms is given in Section *Internal length scale parameters and their relevance in fracture and fatigue*, with their relevance to fracture and fatigue problems. The finite element equations for the theories of Eringen and Aifantis will be given in Section *Finite element discretisation* and demonstrated via a benchmark example in Section *Benchmark example – Strip with central crack*.

OVERVIEW OF PERTINENT GRADIENT ELASTICITY THEORIES

The literature on gradient elasticity theories is very rich, and many different versions of gradient elasticity have been formulated over the past decades. Without attempting to be complete in this overview, some of the theories will be discussed that have had the most impact in the community. The emphasis in the discussion is on how gradient elasticity theories can be formulated with as few additional constitutive parameters as possible.

Mindlin (1964)

In the 1960s, Mindlin formulated a theory of linear elasticity with micro-structure whereby he distinguished between micro-scale deformation and macro-scale deformation. In its most general form, there are over 900 independent constitutive constants, but this was reduced by Mindlin to 18 for isotropic materials [3]. Further simplifications were made by setting the micro-scale deformation equal to the macro-scale deformation. Although Mindlin formulated his theory with the inclusion of inertia terms, the focus here is on statics. The simplest equilibrium equations according to Mindlin's theory can be written as

$$(\lambda + \mu)u_{j,ij} + \mu u_{i,jj} - \ell_1^2(\lambda + \mu)u_{j,ijkk} - \ell_2^2\mu u_{i,jkkk} + b_i = 0 \quad (1)$$

where u_i are the displacements with indices following commas denoting spatial derivatives, λ and μ are the Lamé constants, and b_i are the body forces. The two non-standard parameters, ℓ_1 and ℓ_2 , are internal length scale parameters that account for the micro-structural effects.

Eringen (1983)

Eringen is most renowned for his work in integral nonlocal theories. However, in the 1980s he also derived a differential version of his integral theory, whereby the stresses σ_{ij} satisfy a diffusion-type equation as

$$\sigma_{ij} - \ell^2\sigma_{ij,mm} = C_{ijkl}u_{k,l} \quad (2)$$

where $C_{ijkl} = \lambda\delta_{ij}\delta_{kl} + \mu\delta_{ik}\delta_{jl} + \mu\delta_{il}\delta_{jk}$ and ℓ is a length scale parameter. Eq. (2) is solved together with the equilibrium equations in terms of the stresses as

$$\sigma_{ij,j} + b_i = 0 \quad (3)$$

Eqs. (2) and (3) are a *coupled* set of equations with the stresses and the displacements as independent unknowns. Perhaps unexpectedly, the stresses are the primary unknowns and the displacements act as Lagrange multipliers [6].

Aifantis (1992)

In the 1990s, Aifantis extended his earlier work on the formation of shear bands with finite width in plasticity [7, 8] to elasticity. His model can be considered as a simplification of the Mindlin model by taking $\ell_1 = \ell_2$, which has however important implications for the numerical solution procedure as will be argued below. The field equations, in terms of the displacements, can be rewritten by factorising the various derivatives as



$$\left(1 - \ell^2 \frac{\partial^2}{\partial x_m^2}\right) C_{ijkl} u_{k,jl} + b_i = 0 \quad (4)$$

where ℓ replaces ℓ_1 and ℓ_2 . The factorisation of spatial derivatives allows one to write the original fourth-order differential equations as a set of second-order differential equations [9]. Namely, an additional displacement field u^c can be defined such that Eq. (4) can be rewritten as

$$C_{ijkl} u_{k,jl}^c + b_i = 0 \quad (5)$$

followed by

$$u_k - \ell^2 u_{k,mm} = u_k^c \quad (6)$$

Eq. (5) represents the governing equations of classical elasticity, and their solution u_k^c is used as a source term in Eq. (6). In contrast to Eringen's model, Eqs. (5) and (6) are decoupled. The difference can perhaps best be appreciated by investigation of the two-dimensional equilibrium equations. In Eringen's theory, the equilibrium Eqs (3) are two equations with three unknown stress components, which requires simultaneously solving Eq. (2) to find a solution for the three stress components and two displacement components. On the other hand, in Aifantis' theory the equilibrium Eqs. (5) are two equations with two unknown displacement components, so that this can be solved independently of, and prior to, Eq. (6).

It is also possible [10], and in fact desirable [11], to take the derivatives of Eq. (6) and pre-multiply with the constitutive tensor C_{ijkl} . This yields

$$\sigma_{ij} - \ell^2 \sigma_{ij,mm} = C_{ijkl} u_{k,l}^c \quad (7)$$

which has obviously the same format as Eq. (2) in Eringen's theory, but is related to a different format of the equilibrium equations as explained above. The advantage of using Eq. (7) instead of Eq. (6) is that with the variationally consistent natural boundary conditions of Eq. (7), all singularities are removed from the crack tip, whereas singularities in some strain components remain if Eq. (6) is used [10]. For a detailed discussion on the difference between the theories of Eringen and Aifantis, see [12].

INTERNAL LENGTH SCALE PARAMETERS AND THEIR RELEVANCE IN FRACTURE AND FATIGUE

Compared to classical elasticity, there are two issues that need to be addressed in gradient elasticity. Firstly, the numerical discretisation with finite elements is less straightforward than classical elasticity, which is due to the additional spatial derivatives that are included in the differential equations – this issue will be covered in the next Section. Secondly, through the introduction of the higher-order derivatives additional constitutive coefficients have appeared that must be identified and quantified, which will be discussed briefly in this Section.

Much research effort has been put into linking the internal length scales of gradient elasticity to the lattice geometries of discrete material models; see for instance [13] or [14]. Typically, in such approaches the internal length scales of gradient elasticity are found to be in the order of magnitude of the particle spacing. More recently, the link between homogenisation methods and gradient elasticity has been studied. Homogenisation of a material's response pre-supposes the existence of a so-called Representative Volume Element (RVE), and it has been found in two independent studies [15, 16] that the length scale ℓ of the Aifantis theory is related to the RVE size L_{RVE} via $\ell^2 = L_{RVE}^2 / 12$, and this was also extended to dynamics [17].

As addressed above, the stress and strain singularities around the tips of sharp cracks can be eliminated using gradient elasticity. In fact, in gradient elasticity the stresses and strains are redistributed whereby the length scale parameter sets the size of the area or volume over which this redistribution takes place. The size of the zone with significant gradient activity is thus set by ℓ ; it bears some similarities with the plastic zone ahead of a crack tip and may also be related to the area around the crack tip determined via the Theory of Critical Distances, see for instance the discourse in [18], whilst keeping in mind the relation between gradient elasticity length scales and RVE size mentioned earlier.



FINITE ELEMENT DISCRETISATION

In this Section, finite element discretisations will be presented for the theories of Eringen and Aifantis. The finite element implementation of a slightly different version of the Eringen theory, using strains instead of stresses in Eq. (2), was developed earlier in [6]. A finite element implementation of the Aifantis theory based on Eq. (6) was given in [19] and extended later in [10] to include Eq. (7). However, a unified presentation of implementations of the two theories sheds further light on their commonalities and differences. The index tensor notation used earlier will be exchanged for matrix-vector notation.

Implementation of Eringen's theory

The weak form of Eq. (3) is obtained by pre-multiplying this expression with virtual displacements $\delta \mathbf{u}$ and integration over the domain Ω , that is

$$\int_{\Omega} \delta \mathbf{u}^T \cdot (L^T \boldsymbol{\sigma} + \mathbf{b}) dV = 0 \quad (8)$$

where the differential operator L is defined in the two-dimensional case as

$$L^T = \begin{bmatrix} \frac{\partial}{\partial x} & 0 & \frac{\partial}{\partial y} \\ 0 & \frac{\partial}{\partial y} & \frac{\partial}{\partial x} \end{bmatrix}$$

Integration by parts results in

$$-\int_{\Omega} \delta \boldsymbol{\varepsilon}^T \cdot \boldsymbol{\sigma} dV + \int_{\Omega} \delta \mathbf{u}^T \cdot \mathbf{b} dV + \oint_{\Gamma} \delta \mathbf{u}^T \cdot \mathbf{t} dS = 0 \quad (9)$$

where the virtual strains $\delta \boldsymbol{\varepsilon} = L \delta \mathbf{u}$ and \mathbf{t} are externally applied tractions on the boundary Γ of the domain. The two fields of unknowns, displacements and stresses, are discretised with shape functions N_u and N_{σ} , respectively, by which

$$-\delta \mathbf{u}^T \int_{\Omega} B_u^T N_{\sigma} dV \underline{\boldsymbol{\sigma}} + \delta \mathbf{u}^T \int_{\Omega} N_u^T \mathbf{b} dV + \delta \mathbf{u}^T \oint_{\Gamma} N_u^T \mathbf{t} dS = 0 \quad (10)$$

where $B_u = L N_u$ and underlined vectors contain the discretised nodal values of their continuous counterparts.

The weak form of Eq. (2) is obtained by pre-multiplying with a virtual strain field $\delta \boldsymbol{\varepsilon}$ that is conjugated to the gradient-enriched stress vector $\boldsymbol{\sigma}$ (and therefore in general it holds that $\delta \boldsymbol{\varepsilon} \neq \delta \boldsymbol{\varepsilon}$). Integrating over the domain results in

$$\int_{\Omega} \delta \boldsymbol{\varepsilon}^T \cdot (\boldsymbol{\sigma} - \ell^2 \nabla^2 \boldsymbol{\sigma} - C L \mathbf{u}) dV = 0 \quad (11)$$

where $\nabla^2 = \nabla^T \cdot \nabla$ and the stiffness matrix C contains the elastic moduli of the tensor C_{ijkl} . Integration by parts yields

$$\int_{\Omega} \delta \boldsymbol{\sigma}^T S \boldsymbol{\sigma} dV + \sum_{\xi=x,y} \int_{\Omega} \frac{\partial \boldsymbol{\sigma}^T}{\partial \xi} S \ell^2 \frac{\partial \boldsymbol{\sigma}}{\partial \xi} dV - \int_{\Omega} \delta \boldsymbol{\sigma}^T \cdot L \mathbf{u} dV = 0 \quad (12)$$

where the substitution $\delta \boldsymbol{\varepsilon} = S \delta \boldsymbol{\sigma}$ was made and $S = C^{-1}$ is the (symmetric) compliance matrix. The boundary terms in Eq. (12) have been ignored, which amounts to applying homogeneous natural boundary conditions or setting the spatial gradient of the stresses equal to zero on the boundary. Finite element discretisation gives

$$\delta \boldsymbol{\sigma}^T \int_{\Omega} N_{\sigma}^T S N_{\sigma} dV \underline{\boldsymbol{\sigma}} + \delta \boldsymbol{\sigma}^T \sum_{\xi=x,y} \int_{\Omega} \frac{\partial N_{\sigma}^T}{\partial \xi} S \ell^2 \frac{\partial N_{\sigma}}{\partial \xi} dV \underline{\boldsymbol{\sigma}} - \delta \boldsymbol{\sigma}^T \int_{\Omega} N_{\sigma}^T B_u dV \underline{\mathbf{u}} = 0 \quad (13)$$

For arbitrary test function vectors $\delta \mathbf{u}$ and $\delta \boldsymbol{\sigma}$ Eqs. (10) and (13) form a coupled, symmetric system of equations as



$$\begin{bmatrix} 0 & -K_{u\sigma} \\ -K_{u\sigma}^T & K_{\sigma\sigma} \end{bmatrix} \begin{bmatrix} \underline{u} \\ \underline{\sigma} \end{bmatrix} = \begin{bmatrix} -\underline{f} \\ \underline{0} \end{bmatrix} \quad (14)$$

where the external force vector $\underline{f} = \int N_u^T \underline{b} dV + \oint N_u^T t dS$ and

$$K_{u\sigma} = \int B_u^T N_\sigma dV \quad (15)$$

$$K_{\sigma\sigma} = \int_\Omega \left(N_\sigma^T S N_\sigma + \sum_{\xi=x,y} \frac{\partial N_\sigma^T}{\partial \xi} S \ell^2 \frac{\partial N_\sigma}{\partial \xi} \right) dV \quad (16)$$

As argued in [6], the interpolation functions for stresses and displacements cannot be chosen independently; since the displacements act as Lagrange multipliers, they must be interpolated with polynomials one order lower than the stresses. However, for optimal convergence of the finite element solutions this may not even be enough, as has been demonstrated for classical elasticity implementations of similar format, and more complicated implementations may be necessary [20].

Implementation of Aifantis' theory

For the implementation of the Aifantis theory, Eqs. (5) and (7) are taken. The discretisation of Eq. (7) is the same as that of Eq. (2) from the Eringen theory described above. Eq. (5) is in fact the usual expression of equilibrium in classical elasticity, discretisation of which is very well known and need not be described in detail here. The resulting system of equations can be written as

$$\begin{bmatrix} K_{uu} & 0 \\ -K_{u\sigma}^T & K_{\sigma\sigma} \end{bmatrix} \begin{bmatrix} \underline{u} \\ \underline{\sigma} \end{bmatrix} = \begin{bmatrix} \underline{f} \\ \underline{0} \end{bmatrix} \quad (17)$$

where $K_{uu} = \int B_u^T C B_u dV$, as usual, whilst the other sub-matrices and sub-vectors are the same as in Eq. (14). The main difference between Eqs. (14) and (17) is that the former is *coupled* whereas the latter is *uncoupled*. In particular, this implies that the first row of Eq. (17) can be solved prior to the second row, and that the two sets of interpolation functions can be chosen independently – or indeed the same, which seems the simplest option and has been adopted in [10] and [11], using bilinear quadrilateral elements, as well as [19], using linear triangular elements.

BENCHMARK EXAMPLE – STRIP WITH CENTRAL CRACK

To illustrate the performance of the two theories and their respective finite element implementations, the benchmark problem of a strip with a central crack as shown in Fig. 1 is studied. For reasons of symmetry, only the top-right quarter is analysed, and the strip geometry is set via $L = 1$ mm. The material parameters are taken as Young's modulus $E = 1000$ N/mm², Poisson ratio $\nu = 0.25$ and internal length scale $\ell = 0.1$ mm. The prescribed displacement $\bar{u} = 0.01$ mm.

Following the recommendations in [6], the spatial discretisation of the Eringen model is performed with quadratic shape functions (based on 8-noded quadrilaterals) for the stresses and bilinear shape functions (based on 4-noded quadrilaterals) for the displacements. For the Aifantis model, 4-noded quadrilaterals with bilinear shape functions are used for the stresses as well as for the displacements. Three different mesh densities were used, namely 8×8 , 16×16 and 24×24 elements for the Eringen model, and 16×16 , 32×32 and 48×48 elements for the Aifantis model – the discrepancy is meant to compensate partially for the different interpolation polynomials used for the stresses.

Fig. 2 shows the profiles of the two normal stress components along the horizontal symmetry axis. It is clear that both models predict smooth stress fields with non-singular values at the crack tip: the finite element results converge to unique, finite solutions. There are some minor quantitative differences between the two models, but the most striking difference is probably found in the profile of the vertical normal stress σ_{yy} . In the Eringen model, the gradient-enriched stresses appear in the equilibrium equations, therefore $\sigma_{yy} = 0$ on the crack face. On the other hand, in the Aifantis model the gradient-enriched stresses are computed after resolving the equations of classical elasticity, therefore equilibration with tractions on the crack face does not have to be enforced (although the analyst may choose otherwise).

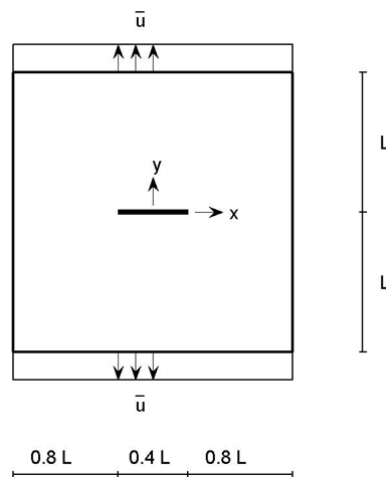


Figure 1: Strip with central crack – geometry and boundary conditions.

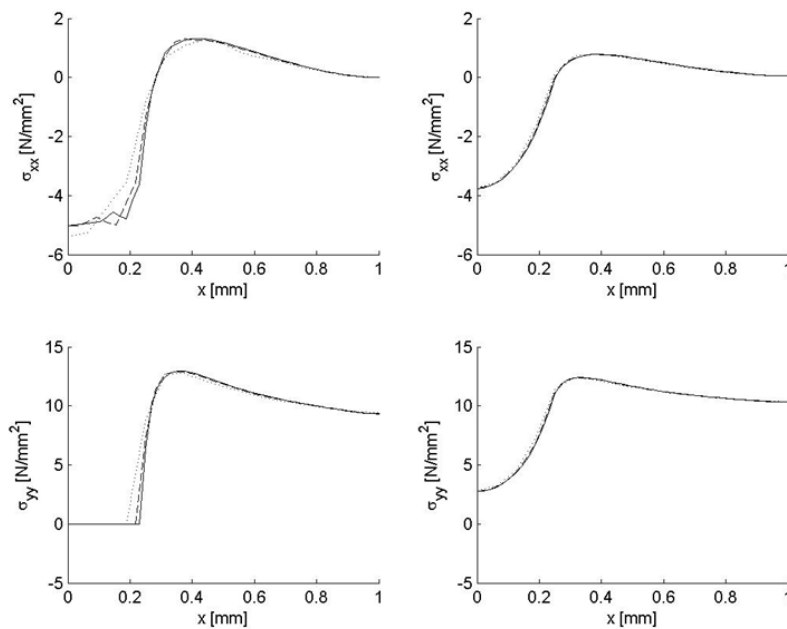


Figure 2: Profiles of normal stresses σ_{xx} (top) and σ_{yy} (bottom) along $y = 0$ for theories of Eringen (left) and Aifantis (right); coarse mesh (dotted), medium mesh (dashed) and fine mesh (solid).

CONCLUSIONS

Different formats of gradient elasticity have been reviewed in this paper, in the context of their relevance for static fracture. The two theories of Eringen and Aifantis share an appealing simplicity in that they each contain only one internal length scale parameter. The relation of the internal length scales with other physical concepts such as the Representative Volume Element or the size of the fracture process zone has been discussed briefly, but warrants further study for the mutual benefit of the two research areas. Finite element implementations have been presented as well, where it must be noted that the Aifantis theory allows for a decoupling of equations, thereby greatly simplifying the spatial discretisation of the governing differential equations. A benchmark problem was used to demonstrate the effectiveness of using gradient elasticity in eliminating the stress singularities around sharp crack tips.



REFERENCES

- [1] A.L. Cauchy, In: *Oeuvres complètes, 1^{re} Série — Tome XI*. Gauthier-Villars, Paris, (1851, reprint 1899) 341.
- [2] W. Voigt, In: *Abhandlungen der Mathematischen Classe der Königlichen Gesellschaft der Wissenschaften zu Göttingen*, 34 (1887) 3.
- [3] R.D. Mindlin, *Arch. Rat. Mech. Analysis*, 16 (1964) 52.
- [4] A.C. Eringen, *J. Appl. Phys.*, 54 (1983) 4703.
- [5] E.C. Aifantis, *Int. J. Engng. Sci.*, 30 (1992) 1279.
- [6] H. Askes and M.A. Gutiérrez, *Int. J. Numer. Meth. Engng.*, 67 (2006) 400.
- [7] E.C. Aifantis, *ASME J. Engng. Mater. Techn.*, 106 (1984) 326.
- [8] E.C. Aifantis, *Int. J. Plast.*, 3 (1987) 211.
- [9] C.Q. Ru, E.C. Aifantis, *Acta Mech.*, 101 (1993) 59.
- [10] H. Askes, I. Morata, E.C. Aifantis, *Comput. Struct.*, 86 (2008) 1266.
- [11] H. Askes, I.M. Gitman, *Int. J. Fract.*, 156 (2009) 217.
- [12] H. Askes, I.M. Gitman, in: *Mechanics of Generalized Continua*, Springer, (2010) 203.
- [13] I.V. Andrianov, J. Awrejcewicz, R.G. Barantsev, *ASME Appl. Mech. Rev.*, 56 (2003) 87.
- [14] A.V. Metrikine, H. Askes, *Phil. Magaz.*, 86 (2006) 3259.
- [15] V.G. Kouznetsova, M.G.D. Geers, W.A.M. Brekelmans, *Int. J. Multiscale Comput. Engng.*, 2 (2004) 575.
- [16] I.M. Gitman, H. Askes, L.J. Sluys, *Fract. Mech. Concr. Struct. Ia-FraMCoS*, (2004), 483.
- [17] I.M. Gitman, H. Askes, E.C. Aifantis, *Int. J. Fract.*, 135 (2005) L3.
- [18] D. Taylor, *Engng. Fract. Mech.*, 75 (2008) 1696.
- [19] L.T. Tenek, E.C. Aifantis, *Comput. Model. Engng. Sci.*, 3 (2002) 731.
- [20] D.N. Arnold, R. Winther, *Numer. Math.*, 92 (2002) 401.